Incorporating Plane-Sweep in Convolutional Neural Network Stereo Imaging for Road Surface Reconstruction

Hauke Brunken and Clemens Gühmann
Chair of Electronic Measurement and Diagnostic Technology, Technical University of Berlin,
Einsteinufer 17, 10587 Berlin, Germany

Keywords: Stereo Vision, Neural Network, Plane Sweep, Pavement Distress.

Abstract: Convolutional neural networks, which estimate depth from stereo pictures in a single step, have become state of the art recently. The search space for matching pixels is hard coded in these networks and in literature is chosen to be the disparity space, corresponding to a search in the cameras viewing direction. In the proposed method, the search space is altered by a plane sweep approach, reducing necessary search steps for depth map estimation of flat surfaces. The described method is shown to provide high quality depth maps of road surfaces in the targeted application of pavement distress detection, where the stereo cameras are mounted behind the windshield of a moving vehicle. It provides a cheap replacement for laser scanning for this purpose.

1 INTRODUCTION

Knowledge about the road surface is useful in several cases, such as road maintenance, driving assistance systems and active suspension systems.

At present for the purpose of road maintenance, specially equipped measuring vehicles are utilized, which use laser scanners to generate a road profile (Eisenbach et al., 2017). Alternatively people are send to observe and measure roads by hand. This is costly and time consuming. As the road surface can change quickly, for example when a pothole develops, the gathered information becomes outdated.

Another subject are driving assistance or autonomous driving systems, where potholes should be circumvented or the driving speed should be reduced due to bad road conditions. Active suspension systems can utilize depth information to provide the best driving comfort.

This work aims at solving the problem of reconstructing the road surface ahead of a moving vehicle by stereo vision. This is a difficult task, as roads have a low texture surface and surface defects produce little change in elevation. The developed system could be mounted on public vehicles, such as public transportation or garbage trucks in order to provide current data for many roads with little effort. Changes in road conditions can be detected early, which can lead to savings in repair costs. While laser scanners capture the world serially, cameras can capture the entire image in parallel. This is advantageous at high driving speeds, as is the case with driver assistance or autonomous driving systems.

The proposed method is an extension of neural networks for disparity estimation by implementing plane sweep stereo into the network. It is trained end-to-end on data, which was created by a more traditional plane sweep approach. The final network learns from the training data and even outperforms the method it learned from in some cases.

Results are shown for the targeted application and are compared to a laser scan.

2 RELATED WORK

Depth estimation from stereo images is a well-known problem (Hartley and Zisserman, 2003), (Szeliski, 2011), (Ikeuchi, 2014). It can be broken down to matching pixels in left and right camera images. The location of a point in 3D space can then be found by triangulation. The corresponding pixel of a pixel in one image lies on the epipolar line in the other image. If the cameras are aligned horizontally, the epipolar line is located in the same row in the second image as the pixel in question in the first image. Traditionally this pixel matching procedure is divided into several stages:

1. If the cameras are not (perfectly) aligned horizon-

Brunken, H. and Gühmann, C.
Incorporating Plane-Sweep in Convolutional Neural Network Stereo Imaging for Road Surface Reconstruction.
DOI: 10.5220/0007352107840791
In *Proceedings of the 14th International Joint Conference on Computer Vision, Imaging and Computer Graphics Theory and Applications (VISIGRAPP 2019)*, pages 784-791
ISBN: 978-989-758-354-4

tally, the pictures are rectified.

2. A similarity measure between each pixel in one image and each pixel on the same horizontal line in the other image is calculated.
3. The similarity measure is used to match pixels of both images. Due to ambiguities, wrong matches can easily occur if only the similarity measure is taken into account. This makes an additional cost function and complex optimization necessary.

Different similarity measures have been utilized. A very efficient one is a convolutional neural network, which outperforms traditional methods like sum of absolute differences, census transform and normalized cross-correlation (Zbontar and LeCun, 2016). This gave rise to the idea of integrating the second and third steps into a single neural network. Different architectures thereof exist. In (Dosovitskiy et al., 2015) a network for estimating optical flow is proposed. That means, a field around a pixel in consecutive frames of a video sequence needs to be searched. If left and right pictures of a stereo camera are used as input, the flow corresponds to disparity. The idea thus was modified for stereo images in (Mayer et al., 2016), where a correlation layer is used to account for the epipolar geometry. In (Kendall et al., 2017) the idea of a cost volume is introduced. First, feature maps for left and right images are calculated in the network. Then feature maps of different disparity levels of one image are stacked on top of the feature maps of the other image. This approach embeds the epipolar geometry. In (Smolyanskiy et al., 2018) a similar network with a semi-supervised training procedure is implemented, which can run near real-time.

Besides Flownet (Dosovitskiy et al., 2015), all these methods search through disparity space, which corresponds to a search in the cameras viewing direction. This creates two problems in the targeted application:

1. Since the cameras are mounted behind the windshield, the angle between the viewing direction of the cameras and the road is sharp. For the task of depth estimation of the surface, many small steps through disparity space are necessary to get a high depth resolution of the surface.
2. The other problem is the rectification of images. To produce a high depth resolution, the baseline between cameras has to be large. This in turn requires the cameras to be tilted in, in order to get an overlap of the images in the region of interest. In this case, rectification can result in a reduction of quality, due to the required stretching and interpolation.

Both problems are solved by the plane sweep approach, which was first introduced in (Collins, 1996): A virtual plane is placed at arbitrary positions in 3D space. Features of both images are projected onto the plane and match if the plane's position is correct. In (Yang et al., 2003) this approach is used to warp entire images for dense scene reconstruction.

In this work, a neural network is extended by a plane sweep approach, in which feature maps are warped by a plane homography inside the network. By projecting the feature map of one camera onto the plane and into the other camera, rectification becomes unnecessary, and, more importantly, by sweeping the virtual plane from below to above the road surface, the search space is reduced. The network is trained on a dataset, which was created by a plane sweep approach in conjunction with semi global matching.

3 METHOD

The method described in this paper consists of an existing convolutional neural network for disparity estimation, which is modified to estimate change in surface elevation by a plane sweep approach. The plane sweep direction is perpendicular to the road surface and therefore a plane must be found which represents the mean road surface. This plane is guessed initially and refined later on.

In this section first the idea of plane sweep and its usage is described. Next, the convolutional neural network on which this work is based on is briefly recapitulated. Subsequently the embedding of plane sweep into this network is described. At the end it is shown how the mean surface can be found.

3.1 Plane Sweep

The left camera image of a plane, that is parallel to the x-y-plane, is calculated by the 2D homography (Collins, 1996)

$$\mathbf{H}_{L,i} = \mathbf{K}_L \begin{bmatrix} \mathbf{r}_{L,1} & \mathbf{r}_{L,2} & z_i\mathbf{r}_{L,3} + \mathbf{t}_L \end{bmatrix}. \qquad (1)$$

$\mathbf{K}_L$ is the camera matrix. The camera location is given by the columns of the rotation matrix $\mathbf{r}_{L,\{1,2,3\}}$ and the translation vector $\mathbf{t}_L$. z_i is the distance between the x-y-plane and the parallel plane.

To find the plane parts of a pair of images was taken of, both images can be back projected onto virtual planes i by the inverse homographies $\mathbf{H}_{L,i}^{-1}$ and $\mathbf{H}_{R,i}^{-1}$, where $\mathbf{H}_{R,i}$ is the homography for the right camera. If the plane is at the correct position for these parts of the images, they will match on the virtual plane. This

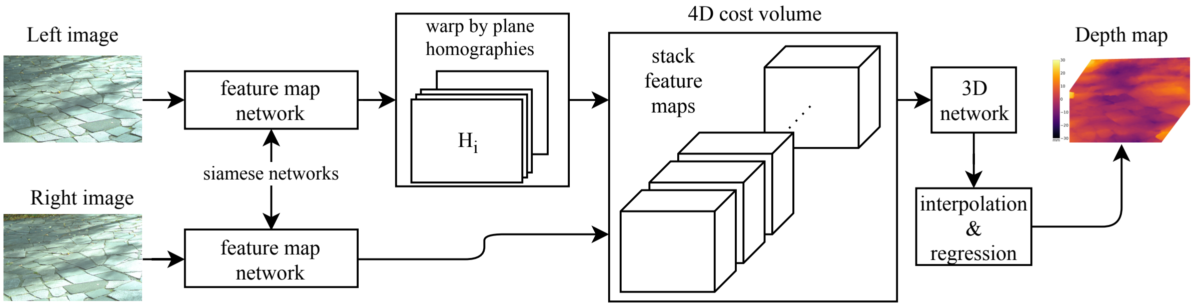

Figure 1: Feature maps are calculated by a Siamese network for both input images. One of them is transformed by a plane homography and a 4D cost volume is created. Matching is done by the 3D network, which outputs the depth map.

idea was introduced in (Collins, 1996), where sparse image features are back projected.

In this work dense feature maps are generated by a neural network. The feature map of the left image is back projected onto virtual planes and projected into the right camera, where matching is performed by the neural network. The back and forth projection is described by

$$\mathbf{H}_i = \mathbf{H}_{R,i} \cdot \mathbf{H}_{L,i}^{-1}. \qquad (2)$$

Performing the matching in the camera space instead of the plane space has several advantages: Images – or feature maps in this case – are not stretched much, which is the case if the virtual plane is not parallel to the camera. The shape of the cost volume stays the same, no matter of the perspective the plane induces. Besides, that way only the feature map of one image has to be transformed.

3.2 Neural Network for Disparity Estimation

Different architectures of neural networks for depth estimation exist, as was laid out in Section 2. The plane sweep extension can be added to all networks which are based on the idea of a cost volume. Here the work of (Chang and Chen, 2018) is incorporated, as it is able to exploit global context information. By creating image features with the help of spatial pyramid pooling, region-level features instead of pixel-level features are introduced (Chang and Chen, 2018). As roads have little texture, it is believed that region-level features will improve the overall performance, especially if cracks or other contexts are visible.

Their network consists of four parts: A Siamese network that creates feature maps from input images at a reduced resolution, concatenation of these feature maps, creating a 4D cost volume, a 3D network, which calculates the cost for each disparity value for every location, upscaling by interpolation, and a regression function. The feature map network gets rectified 3-channel images as input with resolution $W \times H$ (with times height) and creates F feature maps with resolution $W/4 \times H/4$ per image. The cost volume is assembled according to disparity space. That means, for each considered disparity value, the feature maps of the reference image are stacked on top of the shifted feature maps of the other image. This produces a cost volume of dimension $W/4 \times H/4 \times D/4\ x\ 2F$. D is the number of considered disparity values. The 3D network converts the 4D cost volume into a 3D cost volume of dimension $W/4 \times H/4 \times D/4$ by 3D convolutions, which is upscaled by trilinear interpolation to the original resolution of $W \times H \times D$. Now a regression function finds the best fitting disparity value by regressing over the D values at every location. The regression function is

$$\hat{d} = \sum_{d=0}^{D_{max}} d \cdot \sigma(-c_d), \qquad (3)$$

where $\sigma()$ is the softmax operation, d are the disparity values, D_{max} is the maximum disparity and c_d is the cost value.

3.3 Neural Network for Surface Depth Map Estimation

In the proposed method the assembly of the cost volume is altered according to plane sweep. First P planes parallel to the road surface are proposed. The right image is taken as reference, thus the left feature maps need to be warped by the induced homographies. For every proposed plane, the feature maps of the reference image are stacked on top of the warped feature map of the other image. This produces a cost volume of dimension W/4 x H/4 x P x 2F. The 3D network and regression function are left unchanged. The upscaling function changes, as that it does not have to upscale the disparity (plane, respectively) dimension. An overview of the method is shown in Figure 1.

Warping of the feature maps is accomplished by inverse warping (Szeliski, 2011): Coordinates of every pixel of the reference image are transformed by the inverse of the plane induced homography (Equation 2). The result is a lookup table. The feature maps of the left image are copied with the help of this lookup table, which is first rounded to the nearest integer coordinate. As the neural network generates features maps at a lower resolution compared to the input images, the camera matrices have to be scaled before applying Equation 2.

One might be tempted to use a more sophisticated approach as in spatial transformer networks (Jaderberg et al., 2015), where bilinear interpolation is used. In our experiments this does not work. The neural network has a large receptive field (Chang and Chen, 2018), which, in conjunction with interpolation, presumably breaks the relation between an image pixel and its corresponding value in the feature map. During evaluation bilinear interpolation can be utilized.

Training is performed end-to-end on depth maps, with the target being the index of the virtual planes. The usage of the index is similar to the usage of disparity in Section 3.2. That way, the network is independent of the actual depth values and different plane hypothesis can be proposed while training and evaluating.

3.4 Locating the Mean Road Surface

As the plane sweep is conducted from below to above the mean surface, its location has to be known in advance. An initial plane can be guessed, as the approximate positions of the cameras in relation to the road are known. The location is then refined: A depth map is created by the neural network and is then back projected to 3D space, resulting in a 3D point cloud in the camera coordinate system. A grid of points is extracted as a subset to save some calculation time. A plane, which best resembles the point cloud, is then found by a random sample consensus (RANSAC) algorithm (Fischler and Bolles, 1981). In that the mean of the point cloud is subtracted. Singular value decomposition is utilized, which directly gives the rotation matrix from the camera coordinate system to the plane coordinate system, in which the x-y-plane resembles the mean surface. It is located in the center of the road. The subtracted mean is the translation vector. To find the final $\mathbf{r}_{\{L/R\},\{1,2,3\}}$ and $\mathbf{t}_{\{L/R\}}$, which are used in Equation 1, the transformation between camera centers and camera coordinate system has to be accounted for.

To generate a bird's-eye view later, it is useful to place the camera coordinate system in the center between the cameras. The rotation between camera coordinate system and plane can then be composed by a rotation around the x-axis, followed by a rotation around the y-axis. Thus, the rotation matrix is disassembled to Euler angles, the rotation around the z-axis is set to 0 and the rotation matrix is reassembled. This ensures that the birds-eye-view does not get rotated if it is shown in the road coordinate system.

After locating the mean surface, the neural network is evaluated a second time.

4 EXPERIMENTS

In the following section the system setup, the training procedure and the evaluation is described.

4.1 System Setup

Two Basler acA1920-150uc global shutter color cameras with 25 mm lenses are employed. The sensors have an optical size of 2/3” with a resolution of 1920×1200 pixels. The pixel size is $4.8\,\mu\text{m} \times 4.8\,\mu\text{m}$. The cameras are mounted on a rig behind the windshield of a vehicle. As the distance between cameras and road is large (up to 13 m at the upper edge in Figure 2) and the depth resolution needs to be high (elevation differences of a road are in the mm scale), the baseline has to be as large as possible. Due to the flat geometry, a large baseline does not produce occlusions. The baseline is set to 1.08 m and camera height above ground is 1.4 m. In order to have a large overlapping part in both pictures, cameras are tilted in by 6° each. The angle between the camera rig and the road is 13°, in order to look across the hood. This makes it possible to record an area of approximately $2\,\text{m} \times 7\,\text{m}$.

The aperture has a big influence on the depth of field. For the depth of field to be large, it has to be small. On the other hand the aperture influences the required shutter time and thereby the motion blur, thus it has to be large. Even at slow driving speeds the motion blur predominates. For this reason, the aperture is set to the smallest value of f/1.4 for images taken while driving and to f/8.0 for standstill images.

As the windshield has an influence on calibration parameters (Hanel et al., 2016), calibration is performed with the cameras in their final position.

4.2 Training

The proposed convolutional neural network (referred to as CNN in the following) is pretrained on the KITTI 2015 dataset. Therefore, the cost volume in

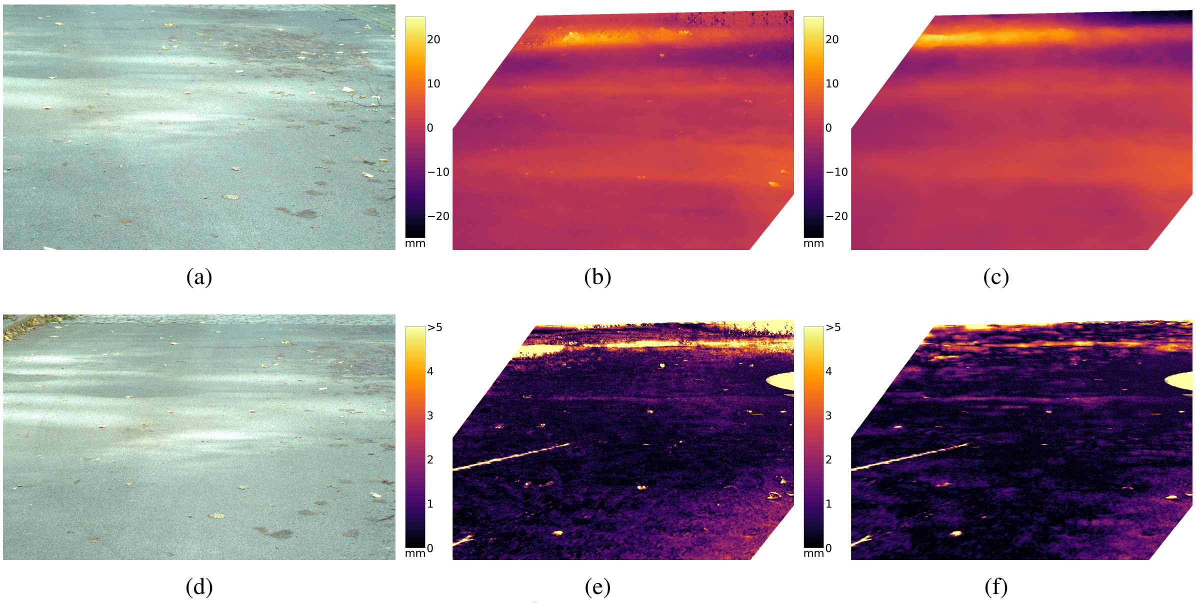

(a) (b) (c)

(d) (e) (f)

Figure 2: Static scene: **a**,**d** left and right image **b**,**c** depth map generated by SGM and CNN method (viewed from the right camera perspective) **e**,**f** error between laser scan reference and SGM/CNN method. The circular part on the right and the stripe on the left are artefacts of the laser scan. The distance between camera and the lower part of the image is 4.5 m, between camera and upper part 13.0 m.

the network is assembled as described in Section 3.2. Learned weights are saved and cost volume assembly is switched to the plane sweep approach (Section 3.3). Training is continued with data of the targeted application. For the training set depth was extracted by a stereo method, which is based on a plane sweep approach in conjunction with semi-global matching (the method is referred to as SGM) and is out of scope of this paper. It is based on the work in (Hirschmüller, 2008). The location of the mean road surface is an output of the earlier method and is also used for training. The training dataset consists of 510 stereo images, which were taken while driving. Another 20 still stereo images were taken outside the vehicle.

Laser scans are not used for training because a sufficiently large data set was not available and is difficult to obtain. Laser scanning and capture of stereo images would have to take place simultaneously and the relationship between scanner and camera would have to be precisely known. This makes the measurement complex and expensive equipment would be necessary, especially for the measurements while driving. Thus, a stereo method is used.

The number of feature maps F is set to 32 and the number of planes P to 64. Plane sweep is performed from -30 mm to $+30$ mm around the mean road surface. An example of a training set composed of left and right color images as input and a depth map as output can be seen in Figure 2a, 2d and 2b (although this particular example was used for validation only).

Training is performed on two NVidia GTX 1080 Ti graphics cards (both have 11 GB of memory) in parallel mode. The model does not fit into memory in training mode if images with the full resolution of 1920×1200 pixels are employed. Thus, 256×256 pixel patches of the right image are randomly chosen. The corresponding patch in the left image can be calculated, as the planes which will be gone through while sweeping are known in advance. The left image patch is padded to 576×300 pixels in order to have a uniform size for the learning batch. The principal points in the camera matrices have to be adjusted according to the patch locations. Batch size is set to 8. In evaluation mode, when no gradients are required and if intermediate results are deleted, the network for full resolution images fits into GPU memory of a single card.

4.3 Evaluation

In order to interpret the results, first the depth resolution of the camera system is investigated. The method is then evaluated by a comparison against a laser scan with standstill images. Afterwards, results from the targeted application of pavement destress detection while driving are shown.

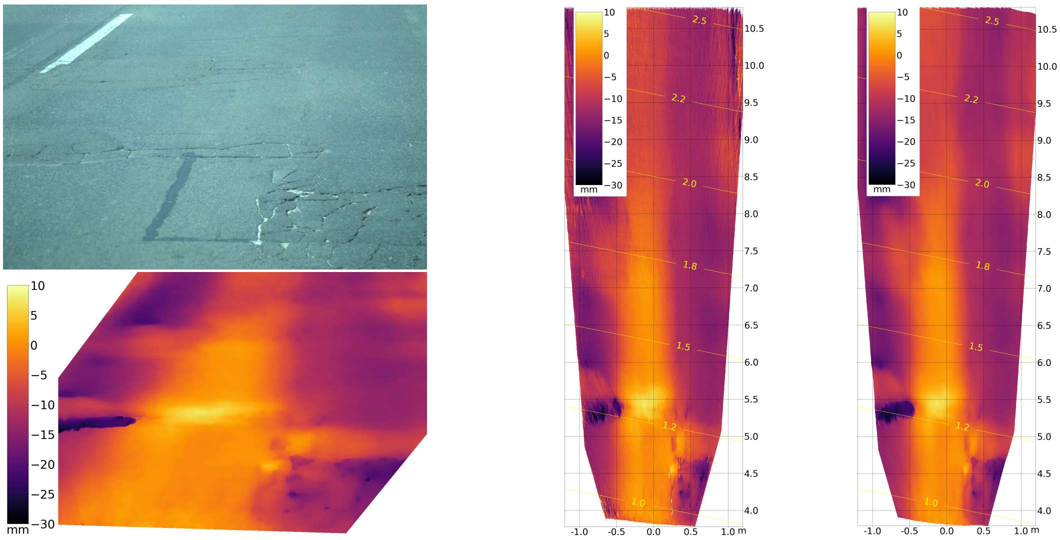

(a) (b) (c)

Figure 3: (a) Right image, captured from behind the windshield of a moving car at 37 km h^{-1} and corresponding depth map created with CNN method, (b) depth map from a bird's-eye view with contour lines, indicating depth resolution in mm/pixel created by SGM method and (c) created by CNN method.

4.3.1 Depth Resolution

For the aforementioned setup, the depth resolution is calculated as follows: If the correct plane is known for a pixel in the right camera image, the matching pixel in the left camera image can be calculated by the plane homography. If the plane is raised, the matching pixel will be shifted. The elevation of the plane divided by the pixel shift is embraced as the resolution. It is shown as contour lines in Figures 3b and 3c and in Figure 4 for the central line between cameras. The exact resolution depends on the relation between cameras and the mean surface.

4.3.2 Comparison Against Laser Scan

As a reference a laser scan was conducted. The scanner (Z+F IMAGER 5006h) has a range uncertainty of 0.4 mm and an uncertainty in vertical and horizontal direction of 0.007°. This sums up to a total maximal uncertainty of 0.8 mm in the direction perpendicular to the road surface in the area of interest. Due to the high precision of the laser scanner, it is considered to be the ground truth.

For comparison, the depth maps are projected to 3D space, where the distance to the point cloud of the laser scanner can be calculated. This is accomplished with the help of the software CloudCompare (GPL software, 2017). Because the relation between camera and laser scanner coordinate system is unknown, the compared point cloud is rotated and shifted until both point clouds line up. Then a piecewise quadratic function is fitted through the reference point cloud and the shortest distance to the compared point cloud is calculated.

The result is shown for standstill images from the right cameras perspective in Figure 2e and 2f for the SGM and CNN methods. SGM refers to the method which was used to create the training data and CNN to the proposed method. Images were taken outside the vehicle while standing still.

It can be seen that both methods are capable of reconstructing the road surface with high precision. The mean absolute error (MAE) is 1.1 mm for SGM and 0.8 mm for the CNN method. The CNN method did not just learn from the SGM method, it even outperforms SGM in this example. SGM fails in particular regions, which can be seen in the upper left and upper right corner, where CNN produces the correct depth according to the error image (Figure 2f) and SGM does not (Figure 2e). The reason presumably is that in the CNN method region-level features are employed (Section 3.2). The SGM method produces correct results for most pixels, while some are wrong. The correct pixels fit the model, which is tried to be learned by the neural network. The wrong pixels appear as noise. Since the correct pixel outweigh the wrong pixels, the neural network is able to generalize the correct and to reject the erroneous training data.

Figure 4 shows the MAE of horizontal lines in bird's-eye view (refer to Figure 3c) for Figure 2 and the physical resolution as described in Section 4.3.1 for the central vertical line. The small MAEs of the entire point clouds compared to the MAEs of hori-

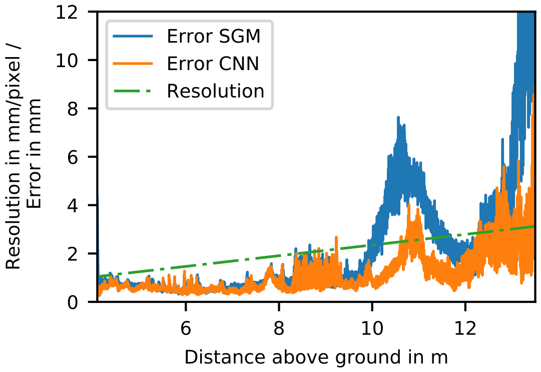

Figure 4: Errors of the SGM and CNN methods compared to the laser scan are shown, which increase over distance from the cameras. The physical depth resolution of the stereo camera setup decreases over distance.

zontal lines shown in the graph are caused by the fact that the density of the point cloud decreases over distance. Thus, there are more points with small errors than with large errors. The mean of MAEs of horizontal lines is 2.1 mm for SGM and 1.2 mm for CNN. The sudden increase of the error at 11 m is caused by the circular artefact of the laser scan (Figure 2e and 2f) and the erroneous section of the SGM method in the upper left (Figure 2e).

Compared to the physical resolution the errors are very small, especially when they are close to the cameras. The methods are capable of achieving subpixel accuracy. The SGM method interpolates between pixels by plane sweeping and image warping, while the CNN method uses the regression function (Equation 3). Another cause is the alignment of point clouds (Section 4.3.2), which reduces the error artificially.

4.3.3 Final Application

Figure 3 shows the right camera image and the corresponding depth maps from the cameras perspective and from a bird's-eye view. The images were taken from behind the windshield while driving at 37 km h^{-1}. A repair patch is visible (covering parts of the lane mark), which is elevated from the road. Closer to the camera on the left hand side a depression can be seen. In the lower right several cracks can be extinguished. If one looks at the bird's-eye view, rutting is visible across the entire distance.

The CNN method (Figure 3c) is more robust than the SGM method (Figure 3b), which can be seen by looking at the lower left and upper right corners. Overall the CNN method produces smoother depth maps.

Figure 5 shows another example at a higher driving speed of 75 km h^{-1}. Although no laser scans are available for images which were taken while driving, the results are qualitatively correct. Please note that the color scales cover different ranges in Figures 2, 3 and 5.

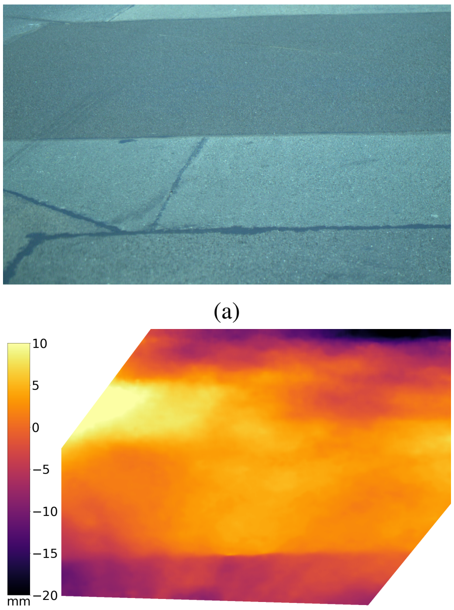
(a)

(b)

Figure 5: (a) Right image, captured from behind the windshield of a moving car at 75 km h^{-1} and (b) corresponding depth map created with the CNN method.

5 CONCLUSION

It was shown how convolutional neural networks for disparity estimation can be adapted to predict depth maps of flat surfaces. Results are compared against a laser scan and show high accuracy over large distances. The new method even outperforms the method it learned from in some cases.

The proposed method proves to be very suitable for the challenging task of road surface reconstruction. It can be utilized to quickly scan road surfaces with little effort at driving speeds.

REFERENCES

Chang, J.-R. and Chen, Y.-S. (2018). Pyramid Stereo Matching Network. *arXiv preprint arXiv:1803.08669*, page 9.

Collins, R. T. (1996). A space-sweep approach to true multi-image matching. In *Computer Vision and Pattern Recognition, 1996. Proceedings CVPR'96, 1996*

IEEE Computer Society Conference on, pages 358–363. IEEE.

Dosovitskiy, A., Fischer, P., Ilg, E., Hausser, P., Hazirbas, C., Golkov, V., van der Smagt, P., Cremers, D., and Brox, T. (2015). Flownet: Learning optical flow with convolutional networks. In *Proceedings of the IEEE International Conference on Computer Vision*, pages 2758–2766.

Eisenbach, M., Stricker, R., Seichter, D., Amende, K., Debes, K., Sesselmann, M., Ebersbach, D., Stoeckert, U., and Gross, H.-M. (2017). How to get pavement distress detection ready for deep learning? A systematic approach. In *2017 International Joint Conference on Neural Networks (IJCNN)*, pages 2039–2047, Anchorage, AK, USA. IEEE.

Fischler, M. A. and Bolles, R. C. (1981). Random sample consensus: a paradigm for model fitting with applications to image analysis and automated cartography. *Communications of the ACM*, 24(6):381–395.

GPL software (2017). Cloudcompare 2.8.

Hanel, A., Hoegner, L., and Stilla, U. (2016). Towards the Influence of a Car Windschield on Depth Calculation with a Stereo Camera System. *ISPRS - International Archives of the Photogrammetry, Remote Sensing and Spatial Information Sciences*, XLI-B5:461–468.

Hartley, R. and Zisserman, A. (2003). *Multiple view geometry in computer vision*. Cambridge University Press, Cambridge, UK; New York.

Hirschmüller, H. (2008). Stereo Processing by Semiglobal Matching and Mutual Information. *IEEE Transactions on Pattern Analysis and Machine Intelligence*, 30(2):328–341.

Ikeuchi, K., editor (2014). *Computer Vision - A Reference Guide*. Springer US, Boston, MA.

Jaderberg, M., Simonyan, K., Zisserman, A., and others (2015). Spatial transformer networks. In *Advances in neural information processing systems*, pages 2017–2025.

Kendall, A., Martirosyan, H., Dasgupta, S., Henry, P., Kennedy, R., Bachrach, A., and Bry, A. (2017). End-to-End Learning of Geometry and Context for Deep Stereo Regression. *arXiv:1703.04309 [cs]*. arXiv: 1703.04309.

Mayer, N., Ilg, E., Hausser, P., Fischer, P., Cremers, D., Dosovitskiy, A., and Brox, T. (2016). A large dataset to train convolutional networks for disparity, optical flow, and scene flow estimation. In *Proceedings of the IEEE Conference on Computer Vision and Pattern Recognition*, pages 4040–4048.

Smolyanskiy, N., Kamenev, A., and Birchfield, S. (2018). On the Importance of Stereo for Accurate Depth Estimation: An Efficient Semi-Supervised Deep Neural Network Approach. *CoRR*, abs/1803.09719.

Szeliski, R. (2011). *Computer Vision*. Texts in Computer Science. Springer London, London.

Yang, R., Welch, G., and Bishop, G. (2003). Real-Time Consensus-Based Scene Reconstruction Using Commodity Graphics Hardware. In *Computer Graphics Forum*, volume 22, pages 207–216. Wiley Online Library.

Zbontar, J. and LeCun, Y. (2016). Stereo matching by training a convolutional neural network to compare image patches. *Journal of Machine Learning Research*, 17(1-32):2.